

Clusters, columns, and lamellae – minimum energy configurations in core softened potentials

Gernot J. Pauschenwein¹ and Gerhard Kahl¹

¹*Center for Computational Materials Science and Institut für Theoretische Physik,
Technische Universität Wien, Wiedner Hauptstraße 8-10, A-1040 Wien, Austria*

(Dated: November 13, 2018)

We give evidence that particles interacting via the simple, radially symmetric square-shoulder potential can self-organize in highly complex, low-symmetry lattices, forming thereby clusters, columns, or lamellae; only at high pressure compact, high-symmetry structures are observed. Our search for these ordered equilibrium structures is based on ideas of genetic algorithms, a strategy that is characterized by a high success rate. A simple mean-field type consideration complements these findings and locates in a semi-quantitative way the cross-over between the competing structures.

PACS numbers: 64.70.Nd, 82.70.Dd, 82.70.-y

“One of the continuing scandals in the physical sciences is that it remains in general impossible to predict the structure of even the simplest crystalline solids from a knowledge of their chemical composition” [1]. Even nowadays, twenty years later, this statement is still valid and it applies equally well to the case that the *physical* properties of the system, e.g., in terms of its inter-particle potential, are known. Indeed, in many problems of hard and soft condensed matter theory a powerful tool that is able to *predict* the ordered equilibrium structures of a system in a reliable way is badly missing. This applies in particular to soft matter systems where particles are able to self-organize in a broad variety of unexpected and often very exotic ordered structures: micellar and inverse micellar structures [2, 3], spirals [4], chains and layers [3, 5], and cluster phases [6, 7] are a few examples.

During the past decades several strategies have been proposed to find the energetically most favorable particle arrangements of a system. Apart from conventional approaches that rely on intuition, experience, or plausible arguments when selecting candidates for ordered equilibrium structures, there are more sophisticated approaches such as simulated annealing [8], basin hopping [9], or meta-dynamics [10]. However, all these strategies are affected by different sorts of deficiencies which can significantly reduce their success rates.

In recent years convincing evidence has been given that search strategies based on ideas of genetic algorithms (GAs) are able to provide a significant break-through to solve this problem. Generally speaking, GAs are strategies that use key ideas of evolutionary processes, such as survival of the fittest, recombination, or mutation, to find optimal solutions for a problem [11]. The wide spectrum of obviously successful applications in different fields of condensed matter physics unambiguously demonstrates their flexibility, reliability, and efficiency: among these are laser pulse control [12], protein folding [13], or cluster formation [14]. In contrast, attempts to apply GAs in the search for ordered equilibrium structures in condensed matter theory were realized considerably later. While the first application probably dates back to 1999 [15]

their widespread use in hard matter theory was pioneered by Oganov and co-workers [16] only recently, where they have become meanwhile a standard tool: a wide spectrum of successful applications ranging from geophysical to technologically relevant problems give evidence of the power and the flexibility of this approach (for an overview see [16]). In *soft* condensed matter theory the usage of these search strategies is still in its infancy. First applications to find minimum energy configurations (MECs) of soft systems have, nevertheless, unambiguously documented the power of the algorithm: successful examples are the identification of exotic lattice structures and cluster phases for particular soft systems [7, 17], or of complex, ordered arrangements of monolayers of binary dipolar mixtures [18]. All these investigations mentioned above give evidence that GA-based search strategies have an extremely high success rate.

In this contribution we consider a simple soft model system, i.e., a square-shoulder system, and show that the GA is an efficient and reliable tool to identify even highly complex MECs in soft matter systems. We discover an overwhelming and undoubtedly unexpected wealth of ordered MECs, which comprise clusters, columns, lamellae, as well as compact structures. The simple shape of the potential allows an easy geometric interpretation of the system’s strategies to form MECs in terms of overlapping shoulders, a nice feature that is not available in systems with continuous potentials. We find evidence that the success rate of our algorithm must be close to 100%.

The square-shoulder system is the simplest representative in the class of the so-called core-softened potentials (for references see [19]). Despite their innocently looking potentials these systems are characterized by a host of surprising properties, such as water-like anomalies [19, 20] or a rich wealth in the occurring structures, investigated in detail in two-dimensional systems [3, 18]. The potential $\Phi(r)$ of the square-shoulder system,

$$\Phi(r) = \begin{cases} \infty & r \leq \sigma \\ \epsilon & \sigma < r \leq \lambda\sigma \\ 0 & \lambda\sigma < r \end{cases}, \quad (1)$$

consists of an impenetrable core of diameter σ with an adjacent, repulsive, step-shaped shoulder of height ϵ and width $\lambda\sigma$. For the aims of the present contribution it represents the 'quintessential' test system [21]. But we also point out that the square-shoulder system is not only of purely academic interest: it represents a reasonable model system for colloidal particles with a core-corona architecture, as has been given evidence for in [22]. Further, we introduce the number-density $\varrho = N/V$, N and V being the number of particles and the volume, respectively.

The MECs for this system have been identified via a GA-based search strategy in the NPT ensemble. For details of the encoding of the individuals (= lattices) and of the reproduction mechanism we refer to [23]. The quality of an individual \mathcal{I} is measured via the fitness function $f(\mathcal{I})$, for which we have chosen $f(\mathcal{I}) = \exp\{-[G(\mathcal{I}) - G_0]/G_0\}$. Since our investigations are restricted to the case $T = 0$, the Gibbs free energy, $G(\mathcal{I})$, reduces at a given pressure P to $G = U + PV$, U being the lattice sum; G_0 is the Gibbs free energy of a reference structure. Significant extensions of the search strategy were required due to the impenetrable core: as a consequence of the highly stochastic character of GAs, the algorithm will propose with a high probability lattices where the cores of the particles overlap: such configurations are unphysical and thus useless. A more *quantitative* investigation reveals that the physically relevant lattices (characterized by non-overlapping cores of the particles) populate only a highly porous subset of the search space [24].

To overcome this problem a suitable modification is urgently required, which guarantees that unphysical configurations are excluded *a priori* so that only lattices with non-overlapping cores are created. Such a strategy has been developed and will be outlined briefly. We start for simplicity with a simple lattice, described via a set of linearly independent vectors \mathbf{a}_1 , \mathbf{a}_2 , and \mathbf{a}_3 . In order to satisfy our expectations, they have to meet several requirements. First, the vectors are chosen such that $|\mathbf{a}_1| \leq |\mathbf{a}_2| \leq |\mathbf{a}_3|$, where $|\mathbf{a}_1|$ represents the shortest possible distance between lattice sites. Then, \mathbf{a}_2 is selected so that $|\mathbf{a}_2|$ is either equal to $|\mathbf{a}_1|$ or represents the second smallest distance encountered between two lattice points. Finally, the third vector, \mathbf{a}_3 , is chosen so that $|\mathbf{a}_3|$ satisfies a similar relation with respect to $|\mathbf{a}_2|$. Of course, the choice of the $\{\mathbf{a}_i\}$ is not unique. If we are able to construct a lattice so that *a priori* $|\mathbf{a}_1| \geq \sigma$, then it is guaranteed by construction that the particles will not overlap. We have succeeded in developing a formalism that is able to create vectors $\{\mathbf{a}_i\}$, that satisfy the above requirements. These constraints lead to inequalities between the Cartesian components of the vectors; these lengthy relations along with a detailed explanation of the algorithm will be described elsewhere [25]. In non-simple lattices overlap can also be caused by the basis particles. Let us assume that the underlying *simple* lattice satisfies above requirements. Then we calculate all

the distances between the particles of this cell and all particles located in the 26 neighboring cells. Let l_0 be the smallest among these distances; if $l_0 < |\mathbf{a}_1|$, then the vectors $\{\mathbf{a}_i\}$ are scaled by a factor $|\mathbf{a}_1|/l_0$, which guarantees that in the entire lattice no particle overlap will occur.

Thermodynamic properties will be presented in standard reduced units: $\varrho^* = \varrho\sigma^3$, $P^* = P\sigma^3/\epsilon$, $U^* = U/(N\epsilon)$, and $G^* = G/(N\epsilon) = U^* + P^*/\varrho^*$. The simple shape of the potential allows us to simplify the search considerably: since for a fixed particle configuration U^* (counting the number of overlapping coronas) is constant, $G^* = U^* + P^*/\varrho^*$ is a straight line of slope $1/\varrho^*$ in the (G^*, P^*) -diagram. The limiting MECs at low and high pressure are easily identified as close-packed spheres, either with diameter $\lambda\sigma$ (corresponding to a slope $1/\varrho_{\min}^* = \lambda^3/\sqrt{2}$) or with diameter σ (corresponding to a slope $1/\varrho_{\max}^* = 1/\sqrt{2}$) – cf. Fig. 1. Any other MEC occurring in this system is characterized by a line of slope $1/\varrho^*$, satisfying $1/\varrho_{\min}^* > 1/\varrho^* > 1/\varrho_{\max}^*$. Thus $G^* = G^*(P^*)$ is a sequence of straight lines. In a first step we determine in the (G^*, P^*) -diagram the intersection point of the two limiting straight lines mentioned above and launch for this P^* -value a GA-search. This leads to a new MEC, characterized by a lower G^* -value, a density ϱ^* , and thus by a new straight line of slope $1/\varrho^*$. Intersecting this line with the previous lines and iterating this strategy, the entire pressure-range can be investigated in an extremely efficient way. From the economic point of view this systematic procedure is very attractive; but it has two additional advantages: (i) there is no risk to 'forget' MECs which easily occurs when working on a finite P^* -grid; and (ii) it avoids a characteristic drawback of GAs that tend to fail in the vicinity of state points that are characterized by competing structures; in the present approach these transition points are determined *exactly* via the intersection of two straight lines.

At each of the intersection points, 1000 to 3000 independent GA-runs with 700 generations, each consisting of 500 individuals, have been performed. Up to twelve particles per unit cell were considered, a number which offers the system sufficient possibilities to form even highly complex structures. Bearing all this in mind, we are confident that the sequence of MECs which we present in the following are complete.

We have considered three values of λ , corresponding to small ($\lambda = 1.5$), intermediate ($\lambda = 4.5$), and long ($\lambda = 10$) shoulder width. For the first case, G^* and U^* , as functions of P^* , are presented in Fig. 1. G^* is, as mentioned above, a sequence of straight lines, while the energy levels of U^* are rational numbers, given by the number of overlapping coronas per particle. For $\lambda = 1.5$, seven MECs can be identified (cf. acronyms in Fig. 1). At low pressure a columnar structure is identified, while for larger P^* -values, the relatively short corona width allows only for compact structures.

For $\lambda = 4.5$, the considerably broader corona offers the system a large variety of strategies to form MECs.

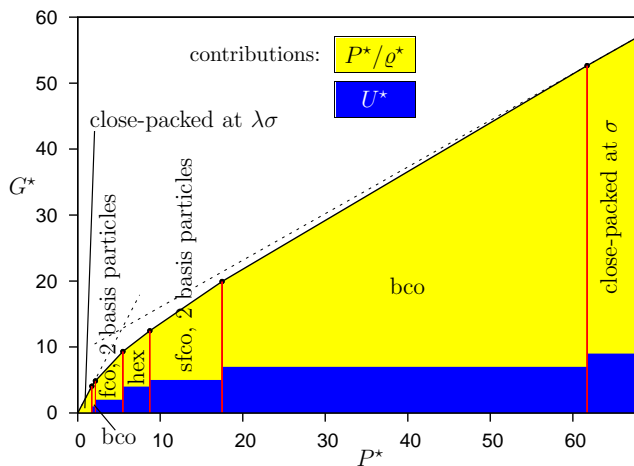


FIG. 1: (color online). G^* and U^* as functions of P^* for the square-shoulder system, $\lambda = 1.5$. Shaded areas represent contributions to G^* as labeled. Broken lines indicate low- and high-pressure limiting cases of MECs (see text).

Their total number amounts to 33 (cf. Fig. 2) which can be grouped with increasing pressure into four structural archetypes: cluster phases, columnar structures, lamellar phases, and, finally, compact structures (see also Fig. 4). At low pressure the system forms cluster crystals, i.e., periodic structures where the lattice points are populated by clusters of particles. A closer analysis reveals a strong interplay between the cluster shape and the cell geometry in the sense that overlaps of coronas of neighboring clusters are avoided. Inside the clusters, which contain up to eight particles, the cores are in direct contact. For demonstration we have depicted in Fig. 3(a) a typical cluster crystal: the equilateral triangle-shaped clusters populate the lattice positions of a single face centered monoclinic structure. As the pressure is increased the system develops a new strategy to minimize G by forming columnar structures. Particles aligned in close or direct contact form single or double stranded columns, which are arranged periodically in space. The inter-columnar spacing is imposed via the width of the corona. An example for the columnar phase is given in Fig. 3(b). As the pressure increases further, the columns are squeezed together in one direction, forming thereby lamellae; the transition scenario is depicted in Fig. 3(c). The lamellar structures are realized in a large variety of morphologies. In Fig. 3(d) we show an example for a lamellar phase: here, two hexagonally close-packed, planar layers are in direct contact and form double layers. Finally, under the influence of the increasing pressure, the lamellae merge, creating in this way typical compact structures.

For $\lambda = 10$, the variety of structures is even richer, in total 48 MECs have been identified. The clusters contain more particles and the columns are more complex in their morphology. For demonstration we depict two of these structures in Figs. 3(e) and (f). However, the sequence

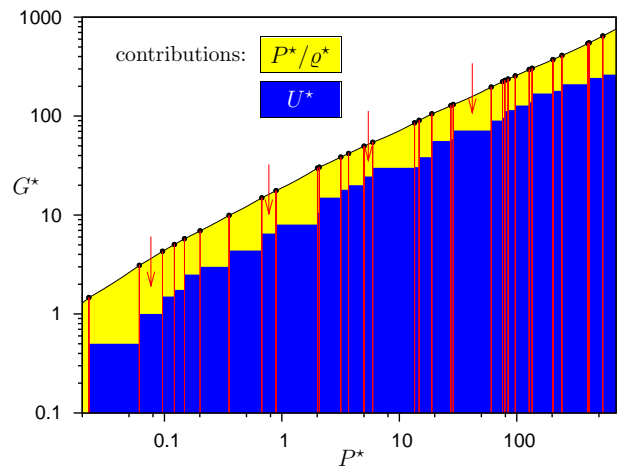


FIG. 2: (color online). G^* and U^* as functions of P^* on a double-logarithmic scale for the square-shoulder system, $\lambda = 4.5$. Shaded areas represent contributions to G^* as labeled. Arrows cf. Fig. 3.

of structural archetypes that has already been identified for $\lambda = 4.5$ is maintained.

The above mentioned transition from clusters to compact structures can be understood on a simple, semi-quantitative level. Generalizing the ideas proposed by Glaser et al. [3] for two dimensional systems, we only consider *aggregates* (i.e., clusters, columns, and lamellae) instead of the individual particles. Assuming an idealized shape for these aggregates (spheres, straight lines, and planes) the inter- and intra-aggregate energy can be calculated. The respective expressions are in some cases rather complex and will be presented elsewhere [25]. G^* is then characterized by ϱ^* , the distance between two aggregates, and their spatial extent. Retaining parameters up to first order and minimizing G^* with respect to these quantities we obtain the thermodynamic properties of the respective phase. In particular, $(U^* + 1/2)/\lambda^3$ as a function of P^*/λ^3 turns out to be λ -independent and has been plotted, along with the respective results obtained via the GA, for all λ -values in Fig. 4. As expected, agreement improves considerably with increasing λ . A detailed analysis of the MECs identified by the GA (in particular for the larger λ 's) reveals, that the MECs populate, according to their aggregate-type, nearly exclusively the respective pressure-range.

Finally, a nice by-product should be mentioned: the well-defined range of the shoulder represents a highly sensitive antenna to discern between competing structures at *close-packed* arrangements. Varying λ from 1 to 4.5, we have identified via analytic considerations not only the usual suspects for close-packed scenarios, namely hcp and fcc; also other, more complicated stacking sequences are observed for particular λ -values – cf. Fig. 5.

Summarizing, our investigations have given *quantitative* evidence about the rich wealth of self-assembly sce-

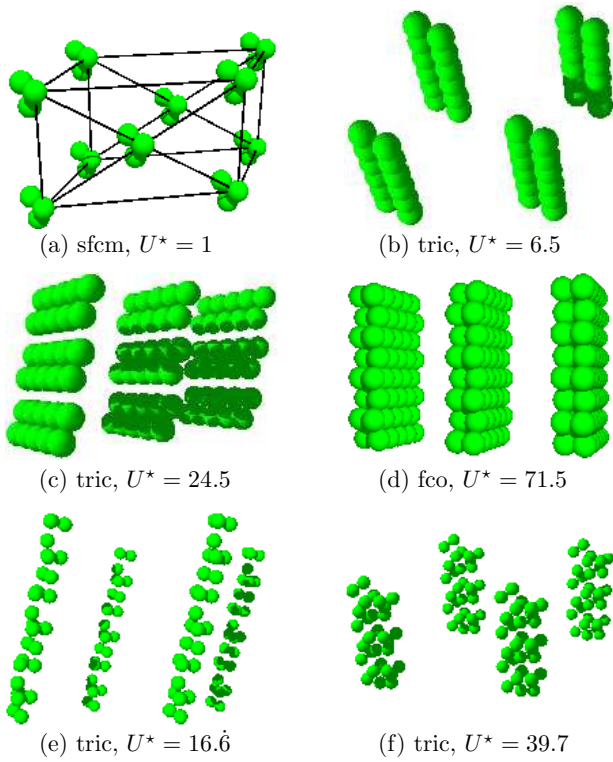


FIG. 3: (color online). Selected MECs for the square-shoulder system with $\lambda = 4.5$ [from (a) to (d)] and with $\lambda = 10$ [from (e) and (f)]. MECs (a) to (d) correspond to pressure values indicated by arrows in Fig. 2.

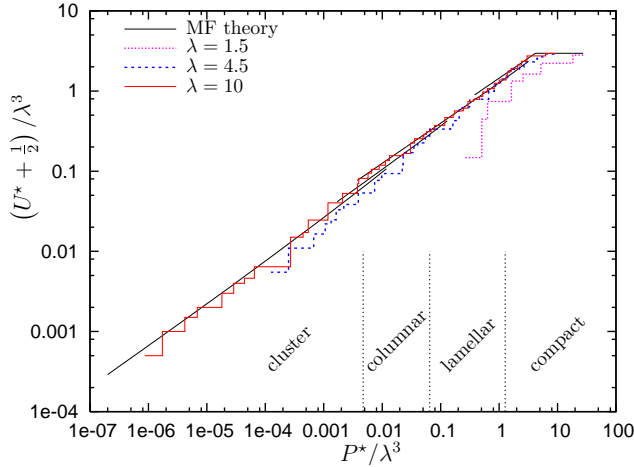


FIG. 4: (color online). Scaled energy per particle $(U^* + 1/2)/\lambda^3$ as obtained via the MF-theory (full black line) and for the three square-shoulder systems investigated (as labeled) as a function of P^*/λ^3 . The vertical, dotted lines indicate the borders of the four different regimes.

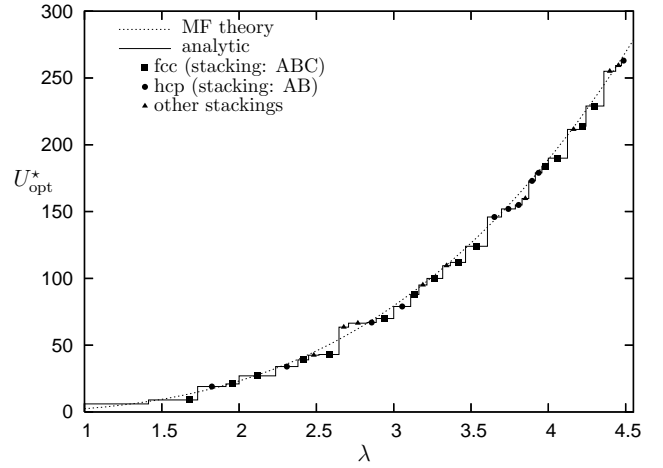


FIG. 5: Minimum number of corona overlaps per particle (U_{opt}^*) and corresponding MECs (as labeled) for close-packed particle arrangements as function of λ , as obtained via analytical considerations and the MF-theory (as labeled). The latter gives $U^*(\varrho^* = \sqrt{2}) = (4\pi\lambda^3/3\sqrt{2}) - (1/2)$.

narios of soft particles that interact via a simple, radially symmetric pair potential: while at high pressure compact structures are dominant, we observe at intermediate and low pressure low-symmetry structures, that include clusters, columns, and lamellae. The simple functional form allows to *understand* fully analytically the system's strategies to self-organize in such complex scenarios. Our findings can also be of technological relevance: since our GA-based search strategy is reliable and efficient, it can easily be applied to systems with more complex interactions, pointing thus towards more technological applications, such as nano-lithography or nano-electricity.

The authors are indebted to Dieter Gottwald and Julia Fornleitner (both Wien) for stimulating discussions. Financial support by the Austrian Science Foundation under Proj. Nos. W004, P17823-N08, and P19890-N16 is gratefully acknowledged.

[1] J. Maddox, Nature **335**, 201 (1988).

[2] C. Pierleoni *et al.*, Phys. Rev. Lett. **96**, 128302-1 (2006).

- [3] M. Glaser *et al.*, Europhys. Lett. **78**, 46004 (2007).
- [4] A. Campbell *et al.*, Phys. Rev. Lett. **94**, 208301 (2005).
- [5] A. de Candia *et al.*, Phys. Rev. E **74**, 010403(R) (2006).
- [6] A. Stradner *et al.*, Nature **432**, 492 (2004).
- [7] B. Mladek *et al.*, Phys. Rev. Lett. **96**, 045701 (2006); *ibid.* **97**, 019901 (2006).
- [8] J. Pannetier *et al.*, Nature **346**, 343 (1990); J. C. Schön and M. Jansen, Angew. Chem. Int. Edit. **35**, 1286 (1996).
- [9] S. Goedecker, J. Chem. Phys. **120**, 9911 (2004).
- [10] R. Martoňák *et al.*, Phys. Rev. Lett. **90**, 075503 (2003); R. Martoňák *et al.*, Nat. Mater. **5**, 623 (2006);
- [11] J. Holland, *Adaption in Natural and Artificial Systems* (The University of Michigan Press, Ann Arbor, 1975).
- [12] A. Assion *et al.*, Science **282**, 919 (1998).
- [13] W.P.C. Stemmer, Nature **370**, 389 (1994).
- [14] D.M. Daeven and K.M. Ho, Phys. Rev. Lett. **75**, 288 (1995).
- [15] S. M. Woodley *et al.*, Phys. Chem. Chem. Phys. **1**, 2535 (1999).
- [16] A. R. Oganov and C. Glass, J. Chem. Phys. **124**, 244704 (2006); J. Phys.-Condens. Mat. **20**, 064210 (2008).
- [17] D. Gottwald *et al.*, Phys. Rev. Lett. **92**, 068301 (2004);
- [18] J. Fornleitner *et al.*, Soft Matter **4**, 480 (2008).
- [19] Z. Yan *et al.*, Phys. Rev. E **73**, 0581601 (2006).
- [20] E.A. Jagla, J. Chem. Phys. **111**, 8980 (1999).
- [21] P. Ziherl and R. Kamien, J. Phys. Chem. B **105**, 10147 (2001).
- [22] Y. Norizoe and T. Kawakatsu, Europhys. Lett. **72**, 583 (2005).
- [23] D. Gottwald *et al.*, J. Chem. Phys. **122**, 074903 (2005).
- [24] For two dimensional simple lattices the parameter space is two-dimensional. Here, the region that corresponds to unphysical, i.e., overlapping particle configurations can be identified rather easily: it is given by infinitely many circles which become for $\rho\sigma^2$ the so-called Ford circles; the latter represent a super-set of the Apollonian Gasket, i.e., an object of fractal dimension of 1.3057.
- [25] G. J. Pauschenwein and G. Kahl (to be published).